

1137  
Eugene C. Lundquist

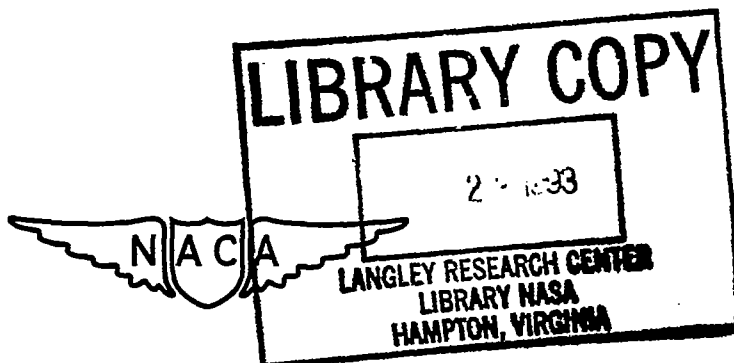
# NATIONAL ADVISORY COMMITTEE FOR AERONAUTICS

TECHNICAL NOTE

No. 1137

DEVICE FOR MEASURING PRINCIPAL CURVATURES AND PRINCIPAL STRAINS  
ON A NEARLY PLANE SURFACE

By A. E. McPherson  
National Bureau of Standards



Washington  
February 1947



NATIONAL ADVISORY COMMITTEE FOR AERONAUTICS

TECHNICAL NOTE NO. 1137

DEVICE FOR MEASURING PRINCIPAL CURVATURES AND PRINCIPAL STRAINS  
ON A NEARLY PLANE SURFACE

By A. E. McPherson

SUMMARY

A device is described which makes possible the measurement of principal extreme fiber bending strains over a circular area having a radius of 0.94 inch with a systematic error on 0.1-inch sheet of the order of  $\pm 0.00003$ . The device requires a Tuckerman autocollimator to measure curvatures along three lines  $120^\circ$  apart and three 1-inch Tuckerman strain gages to measure strains along three other lines  $120^\circ$  apart.

Equations are presented for computing median fiber strains from the measured curvatures and strains at the surface and from the thickness of the sheet.

INTRODUCTION

In static tests of aircraft structures it is frequently desired to determine the magnitude and direction of principal strains and stresses at the median surface of stress-carrying sheet or plate. The usual procedure is to determine extreme fiber strains along at least three gage lines common to both inner and outer surfaces of the plate. The median fiber strains along the three or more gage lines are then equal to the average of the inner and outer extreme fiber strains along these gage lines. The principal strains at the median surface are then computed from well-known equations for rosettes (references 1 and 2). The principal stresses are obtained by substituting the principal strains in the equations expressing Hooke's law for plane stresses (references 1 and 2).

Occasionally it is impossible to measure strains at the inner surface of the plate, either because of inaccessibility or because of the failure of inaccessible strain gages mounted on the inner surface to operate satisfactorily. In such cases it is desirable to determine the principal

stresses at the median surface from measurements on the outer surface of the plate only. The device described in this report was developed for this purpose at the request of the Bureau of Aeronautics, Navy Department.

The author wishes to express his appreciation to the Navy Department for releasing this report for publication.

#### PRINCIPLE OF OPERATION OF THE DEVICE

The device is designed to measure curvatures and strains on the surface of a plate along two sets of gage lines; each set consisted of three gage lines  $120^\circ$  apart. From the curvatures and the thickness of the plate it is possible to compute extreme fiber bending strains along the strain gage lines. Subtracting these from the total strains at the extreme fiber gives the median fiber strains along the three gage lines  $120^\circ$  apart. The principal strains and stresses and their direction may be computed from these three values of median fiber strain as explained in references 1 and 2.

One portion of the device, that for measuring strains at the surface of the plate, is identical with the adaptor for measuring principal strains with Tuckerman strain gages which was described in reference 3. The remaining portion, for measuring principal curvatures, is new.

A photograph of the complete adaptor is shown in figure 1. A diagrammatic sketch is shown in figure 2. The device provides a means of measuring displacements  $\alpha$ ,  $\beta$ ,  $\gamma$  of three points A, B, and C, figure 2a, along three lines  $r_a$ ,  $r_b$ ,  $r_c$ ,  $120^\circ$  apart relative to the center of the device O. As explained in reference 3 the average strains  $e_a$ ,  $e_b$ ,  $e_c$  in the directions  $r_a$ ,  $r_b$ ,  $r_c$  are related to the displacements  $\alpha$ ,  $\beta$ ,  $\gamma$ , by

$$\left. \begin{aligned} e_a &= (2/3r) [\alpha + (\beta + \gamma)/4] \\ e_b &= (2/3r) [\beta + (\alpha + \gamma)/4] \\ e_c &= (2/3r) [\gamma + (\alpha + \beta)/4] \end{aligned} \right\} \quad (1)$$

where  $r$ , the distance from O to A, B, or C, is 0.940 inch. The device also provides a means of measuring the rises  $\delta$ ,  $\epsilon$ ,  $\phi$  (taken positive when in the direction towards the gage) of three points D, E, F, (fig. 2b), with respect to the plane through the points A, B, C. The average curvatures between points A, B, C are then

$$\left. \begin{aligned} \frac{1}{R_{AB}} &= \frac{8\epsilon}{3r^2} \\ \frac{1}{R_{BC}} &= \frac{8\phi}{3r^2} \\ \frac{1}{R_{AC}} &= \frac{8\delta}{3r^2} \end{aligned} \right\} \quad (2)$$

The corresponding extreme fiber bending strains in the direction AB, BC, and CA, on a plate of thickness  $h$  are obtained by multiplying the curvatures by  $h/2$ :

$$\left. \begin{aligned} e_{AB} &= \frac{4h\epsilon}{3r^2} \\ e_{BC} &= \frac{4h\phi}{3r^2} \\ e_{AC} &= \frac{4h\delta}{3r^2} \end{aligned} \right\} \quad (3)$$

The principal extreme fiber bending strains  $e_u''$ ,  $e_v''$  and the angle  $\theta''$  between the direction of  $e_u''$  and the direction of the line BC can be computed as outlined in the appendix (fig. 3 indicates positive value for  $\theta''$ ) by computing the strain differences and the sums:

$$\left. \begin{aligned} t_1'' &= e_{BC} - e_{CA} \\ t_2'' &= e_{CA} - e_{AB} \\ t_3'' &= e_{AB} - e_{BC} \\ S'' &= \frac{1}{3} (e_{BC} + e_{CA} + e_{AB}) \\ T'' &= \frac{\sqrt{2}}{3} \sqrt{t_1''^2 + t_2''^2 + t_3''^2} \end{aligned} \right\} \quad (4)$$

and substituting these in

$$\left. \begin{aligned} e''_u &= S'' + T'' \\ e''_v &= S'' - T'' \\ \tan 2\theta'' &= \frac{\sqrt{3} t''_2}{t''_1 - t''_3} \end{aligned} \right\} \quad (5)$$

The principal curvatures may be obtained by dividing the principal strains by  $h/2$ :

$$\left. \begin{aligned} \frac{1}{R_u} &= \frac{2}{h} e''_u \\ \frac{1}{R_v} &= \frac{2}{h} e''_v \end{aligned} \right\} \quad (6)$$

The directions of principal curvature coincide with the directions of principal strain given by  $\theta''$  in (5).

The extreme fiber bending strains in the direction  $r_a, r_b, r_c$ , may be computed from the quantities defined in (4), as explained in the appendix, with the result:

$$\left. \begin{aligned} e''_a &= S'' + \frac{(t''_3 - t''_1)T''}{2 \sqrt{t''_1{}^2 - t''_1 t''_3}} \\ e''_b &= S'' + \frac{(t''_1 + 2t''_2)T''}{2 \sqrt{t''_1{}^2 - t''_1 t''_3}} \\ e''_c &= S'' + \frac{(t''_1 - t''_2)T''}{2 \sqrt{t''_1{}^2 - t''_1 t''_3}} \end{aligned} \right\} \quad (7)$$

The median fiber strains in the direction  $r_a, r_b, r_c$  are obtained by subtracting (7) from (1)

$$\left. \begin{aligned} e_a' &= e_a - e_a'' \\ e_b' &= e_b - e_b'' \\ e_c' &= e_c - e_c'' \end{aligned} \right\} \quad (8)$$

The principal median fiber strains  $e_u'$ ,  $e_v'$  and the angle  $\theta'$  between the direction of  $e_u'$  and of  $e_a$  (fig. 3 indicates positive value for  $\theta'$ ) are computed finally by repeating the procedure of equations (4) and (5), that is, computing first

$$\left. \begin{aligned} t_1' &= e_a' - e_b' \\ t_2' &= e_b' - e_c' \\ t_3' &= e_c' - e_a' \\ S' &= \frac{1}{3} (e_a' + e_b' + e_c') \\ T' &= \frac{\sqrt{2}}{3} \sqrt{t_1'^2 + t_2'^2 + t_3'^2} \end{aligned} \right\} \quad (9)$$

and substituting these values in

$$\left. \begin{aligned} e_u' &= S' + T' \\ e_v' &= S' - T' \\ \tan 2\theta' &= \frac{\sqrt{3} t_2'}{t_1' - t_3'} \end{aligned} \right\} \quad (10)$$

#### CONSTRUCTION OF THE DEVICE

The construction of the device is shown in the detail and assembly drawings, figures 4 to 8, as well as in the photograph (fig. 1). The device at B, figure 1, the adaptor for measuring the rise at the midpoints of the lines connecting the points A, B, and C (fig. 2b). The rise is measured as the change in angle between a lever and the plane established by

the points A, B, and C (fig. 2b). The angle is measured by a Tuckerman autocollimator as the angle between the fixed mirror C and the lever mirror D (fig. 1).

A satisfactory procedure for assembling part A, figure 1, for measuring surface strains is described in reference 3. A satisfactory procedure for assembling part B, figure 1, for measuring curvature is as follows. First assemble the optical portion of the rise measuring system. The prism housing (7) (fig. 7) is mounted on its pivots with adjusting nut (14) and spring (18) as shown in figures 1 and 4. The housing is rotated on its pivots until its top is parallel to the top of the body (1). A prism (20) is now mounted in the housing, using a suitable cement, so that its diagonal face is parallel to the axis of rotation of the housing and its upper face parallel to the top of the body (1). A similar procedure is followed for mounting the prism (10) in the lever subassembly (fig. 8). The prism housing (7) and the lever (5) is removed from the body (1) and the body is attached to the base (10) by the screw (17) and the dowels (11). The prism housing (7) and lever (5) is then reassembled in the body (1) and the spring bar (9) is inserted. The spring (19) is then installed between this bar and the spring pin (8) on the lever and is adjusted by stretching. When properly adjusted, the force required to move the foot of the lever into contact with base (10), figure 5, should be between 0.002 and 0.005 pound.

#### CALIBRATION OF THE DEVICE

The calibration of the part for measuring surface strains is given in reference 3.

The part for measuring curvature was calibrated as follows. A micrometer screw was so mounted that it could raise or lower the foot of a lever by known amounts. Simultaneous readings were then taken of the change in angle of the lever, as measured by a Tuckerman autocollimator, and the rise of the foot of the lever as measured by the micrometer screw. The calibration curve is shown in figure 9. It is evident that all the levers have the same calibration and that the rise of the lever foot in inches is nearly equal to the change in angle of the lever in radians. Consideration of the geometry of the lever and prism (fig. 9) shows that the relation between rise and change in angle  $\Delta$  of the lever from the plane determined by the points A, B, and C (fig. 2), is

$$\text{Rise} = \Delta - 0.163 \Delta^2 \quad (11)$$

The observed values of rise in general differed from those computed by substituting the measured change in angle into equation (11) by less

than the observational error of 0.0002 inch of the micrometer screw. The rise is given with an error of less than 1 percent by the linear relation

$$\text{Rise} = \Delta \quad (12)$$

for changes  $\Delta$  in angle from the horizontal of less than 0.06 radian.

The rises,  $\epsilon$ ,  $\phi$ ,  $\delta$  of the feet of the levers determined from the measured changes in angle by equation (12) are substituted in equation (3) with  $r = 0.940$  to give the extreme fiber bending strains  $e''$ :

$$e'' = 1.5h \Delta \quad (\Delta \leq 0.06) \quad (13)$$

Substituting  $\Delta = 0.06$  in this equation and solving for  $h$  shows that equation (13) holds within 1 percent, provided

$$h \geq 11e'' \quad (14)$$

Equation (13) holds for strains up to 0.008 (equal to or greater than the yield strain for most metals), provided the sheet thickness exceeds 0.09 inch.

#### ACCURACY OF THE DEVICE

Reference 3 gives an estimate of the accuracy with which surface strains may be measured with the device on a surface which remains nearly flat during the test. An estimate of the accuracy with which the device indicates extreme fiber bending strains was obtained by comparing strains measured by the device with strains measured directly by Tuckerman strain gages.

Two specimens were used. The first was an 0.187- by 3- by 27-inch strip of 24S-T aluminum alloy, supported at the quarter points and loaded at the ends. The uniformity of extreme fiber bending strain near the middle of this strip was checked by Tuckerman strain gages. The strain was found to vary less than 1 percent over the middle 5 inches of the strip. The longitudinal and transverse extreme fiber bending strain at the center of the strip was then measured by Tuckerman strain gages and by the curvature device in two different attitudes with the results shown in figure 10. The extreme fiber bending strains as measured by the device agreed with those measured by the Tuckerman gages within 2 percent of the maximum strain of 0.0020.



The second specimen was an 0.126- by 7.2- by 7.2-inch plate of 24S-T aluminum alloy supported at two diagonally opposite corners and loaded on the other two corners. (See fig. 11.) The loaded plate bent to form a saddlelike surface. The extreme fiber bending strain near the center was measured by pairs of Tuckerman gages and by the curvature device in two different attitudes. The results are shown in figure 11. The extreme fiber bending strains measured by the curvature device agreed with those measured by the Tuckerman gages within 4 percent of the maximum strain, of 0.0008.

In both tests (figs. 10 and 11) it is observed that the specimen became stiffer as the load increased. This increase in stiffness was ascribed to the increase in the effective moment of inertia as the deflection of the plate became comparable with its thickness.

#### CONCLUSIONS

The device described is satisfactory for measuring principal extreme fiber bending strains over an equilateral triangle 1.63 inches on a side with a systematic error not exceeding 2 percent and a mean observational error in strain on 0.1-inch sheet of the order of  $\pm 0.00003$ , with a maximum of the order of 0.00004. The device incorporates as an integral part an adaptor previously described for measuring principal surface strains with a systematic error not exceeding 4 percent. Equations are presented for computing median fiber strains from the measured bending and surface strains.

National Bureau of Standards,  
Washington, D.C., July 14, 1945.

## APPENDIX

DETERMINATION OF MEDIAN FIBER STRAINS  
FROM EXTREME FIBER STRAINS AND CURVATURES

Consider given the total extreme fiber strains

$$\left. \begin{aligned} e_a &= e_{90} \\ e_b &= e_{210} \\ e_c &= e_{330} \end{aligned} \right\} \quad (A1)$$

where the subscripts 90, 210, and 330 denote the angle in degrees relative to a base line BC (fig. 3), and also, the extreme fiber bending strains

$$\left. \begin{aligned} e''_{BC} &= \frac{4h\phi}{3r^2} = e''_0 \\ e''_{CA} &= \frac{4h\phi}{3r^2} = e''_{120} \\ e''_{AB} &= \frac{4h\phi}{3r^2} = e''_{240} \end{aligned} \right\} \quad (A2)$$

The median fiber strains along lines  $r_a$ ,  $r_b$ ,  $r_c$ , are

$$\left. \begin{aligned} e'_{90} &= e_{90} - e''_{90} \\ e'_{210} &= e_{210} - e''_{210} \\ e'_{330} &= e_{330} - e''_{330} \end{aligned} \right\} \quad (A3)$$

where  $e''_{90}$ ,  $e''_{210}$ ,  $e''_{330}$  denote the extreme fiber bending strains along these gage lines.

The extreme fiber bending strains  $e_{10}''$ ,  $e_{210}''$ ,  $e_{330}''$  are computed from  $e_0''$ ,  $e_{120}''$ ,  $e_{240}''$  by determining first the principal extreme fiber bending strains  $e_u''$ ,  $e_v''$  and their direction  $\theta''$  and then determining  $e_{10}''$ ,  $e_{210}''$ ,  $e_{330}''$  from  $e_u''$ ,  $e_v''$ ,  $\theta''$ . In carrying out the computation it is convenient to introduce,

$$\left. \begin{aligned} t_1'' &= e_0'' - e_{120}'' \\ t_2'' &= e_{120}'' - e_{240}'' \\ t_3'' &= e_{240}'' - e_0'' \\ S'' &= \frac{1}{3} (e_0'' + e_{120}'' + e_{240}'') \\ T'' &= \frac{\sqrt{2}}{3} \sqrt{t_1''^2 + t_2''^2 + t_3''^2} \end{aligned} \right\} \quad (A4)$$

The principal strains are then from (equation (2) of reference 3)

$$\left. \begin{aligned} e_u'' &= S'' + T'' \\ e_v'' &= S'' - T'' \end{aligned} \right\} \quad (A5)$$

and the principal direction is given by

$$\tan 2\theta'' = \frac{\sqrt{3} (e_{120}'' - e_{240}'')}{2e_0'' - e_{120}'' - e_{240}''} = \frac{\sqrt{3} t_2''}{t_1'' - t_3''} \quad (A6)$$

Strains along the gage line  $\theta_1$  are related to the principal strains  $e_u''$ ,  $e_v''$  by (reference 4)

$$\left. \begin{aligned} e_{\theta_1}'' &= e_u'' \cos^2 (\theta_1 - \theta'') + e_v'' \sin^2 (\theta_1 - \theta'') \\ &= \frac{e_u'' + e_v''}{2} + \frac{e_u'' - e_v''}{2} \cos 2 (\theta_1 - \theta'') \end{aligned} \right\} \quad (A7)$$

From (A5)

$$\left. \begin{aligned} \frac{e_u'' + e_v''}{2} &= S'' \\ \frac{e_u'' - e_v''}{2} &= T'' \end{aligned} \right\} \quad (A8)$$

Expanding  $\cos 2(\theta_1 - \theta'')$ :

$$\cos 2(\theta_1 - \theta'') = \cos 2\theta_1 \cos 2\theta'' + \sin 2\theta_1 \sin 2\theta'' \quad (A9)$$

where

$$\left. \begin{aligned} \cos 2\theta'' &= \frac{1}{\sqrt{1 + \tan^2 2\theta''}} \\ \sin 2\theta'' &= \frac{\tan 2\theta''}{\sqrt{1 + \tan^2 2\theta''}} \end{aligned} \right\} \quad (A10)$$

Inserting (A6) and noting from (A4) that

$$t_1'' + t_2'' + t_3'' = 0 \quad (A11)$$

gives

$$\cos 2\theta'' = \frac{t_1'' - t_3''}{\sqrt{2 t_2''^2 - t_1'' t_3''}} \quad (A12)$$

$$\sin 2\theta'' = \frac{\sqrt{3} t_2''}{\sqrt{2 t_2''^2 - t_1'' t_3''}} \quad (A13)$$

Inserting (A8), (A9), (A12), and (A13) in (A7) gives

$$e_{\theta 1}'' = S'' + \frac{T''}{\sqrt{2 t_2''^2 - t_1'' t_3''}} \left[ (t_1'' - t_3'') \cos 2\theta_1 + \sqrt{3} t_2'' \sin 2\theta_1 \right] \quad (A14)$$

Letting  $\theta_1 = 90^\circ$ ,  $210^\circ$ , and  $330^\circ$  gives

$\theta_1$	$90^\circ$	$210^\circ$	$330^\circ$	}	(A15)
$\cos 2\theta_1$	$-1$	$1/2$	$1/2$		
$\sin 2\theta_1$	$0$	$\sqrt{3}/2$	$-\sqrt{3}/2$		

$e_{90}'' = S'' + \frac{t_3'' - t_1''}{2 \sqrt{t_2''^2 - t_1'' t_3''}} T''$	}	(A16)
$e_{210}'' = S'' + \frac{t_1'' + 2t_2''}{2 \sqrt{t_2''^2 - t_1'' t_3''}} T''$		
$e_{330}'' = S'' + \frac{t_1'' - t_2''}{2 \sqrt{t_2''^2 - t_1'' t_3''}} T''$		

Inserting (A16) in (A3) gives the desired median fiber strains along the lines  $r_a$ ,  $r_b$ ,  $r_c$ .

#### REFERENCES

1. Osgood, Wm. R., and Sturm, Rolland G.: The Determination of Stresses from Strains on Three Intersecting Gage Lines and Its Application to Actual Tests. Nat. Bur. of Standards, Jour. Res., vol. 10, May 1933, pp. 685-692.
2. Osgood, Wm. R.: Determination of Principal Stresses from Strains on Four Intersecting Gage Lines  $45^\circ$  Apart. Nat. Bur. of Standards, Jour. Res., vol. 15, Dec. 1935, pp. 579-581.
3. McPherson, A. E.: Adaptor for Measuring Principal Strains with Tuckerman Strain Gage. NACA TN 898, 1943.
4. Love, A. E. H.: A Treatise on the Mathematical Theory of Elasticity. Univ. Press (Cambridge, Eng.), 1920.

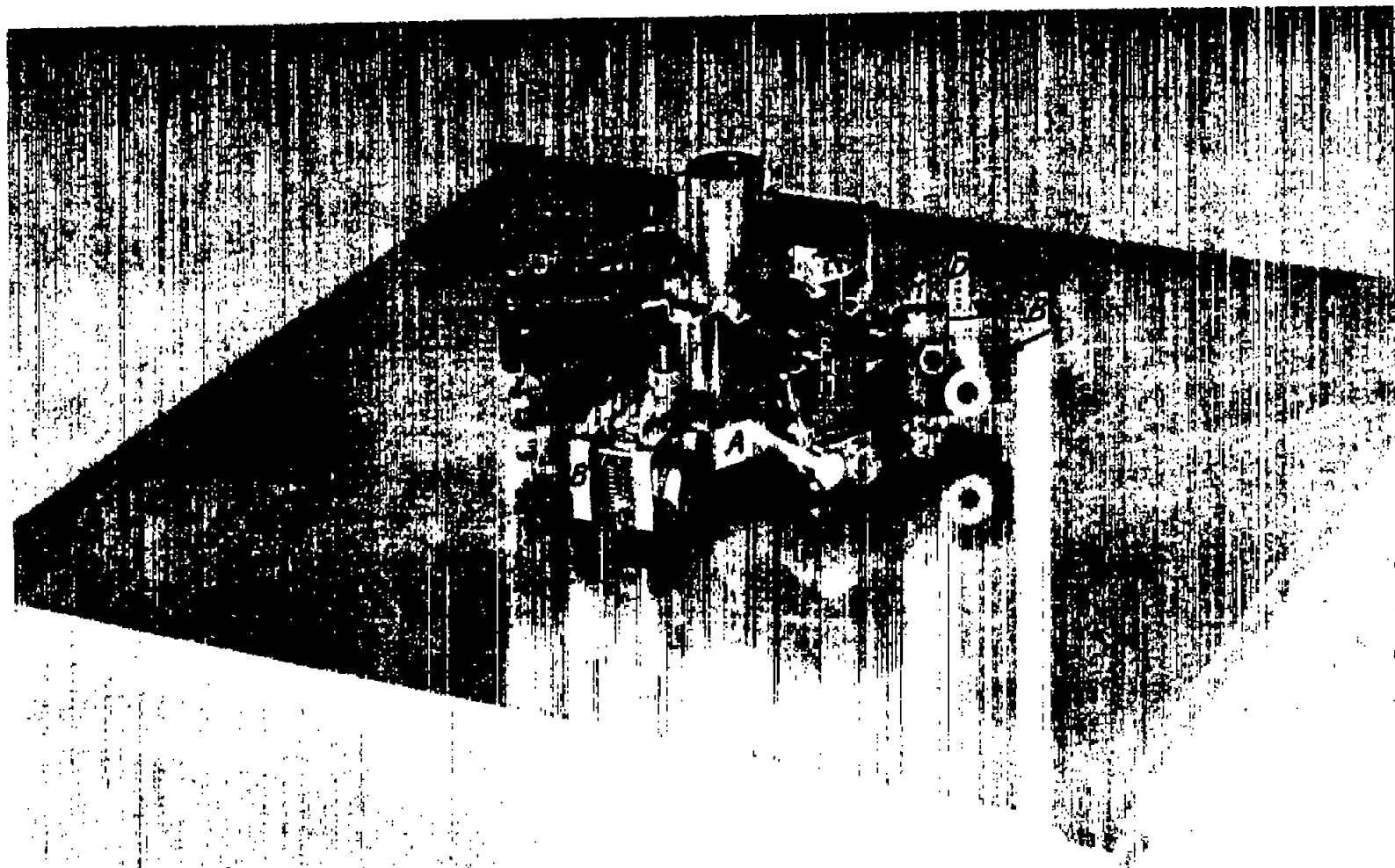


Figure 1.- Complete adaptor.

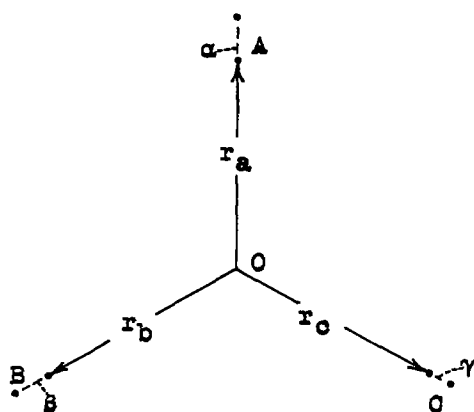


Figure 2a.- Strain measurements.

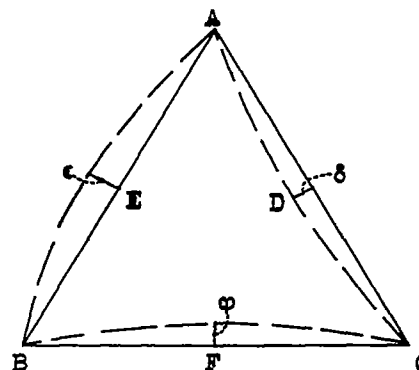


Figure 2b.- Curvature measurements.

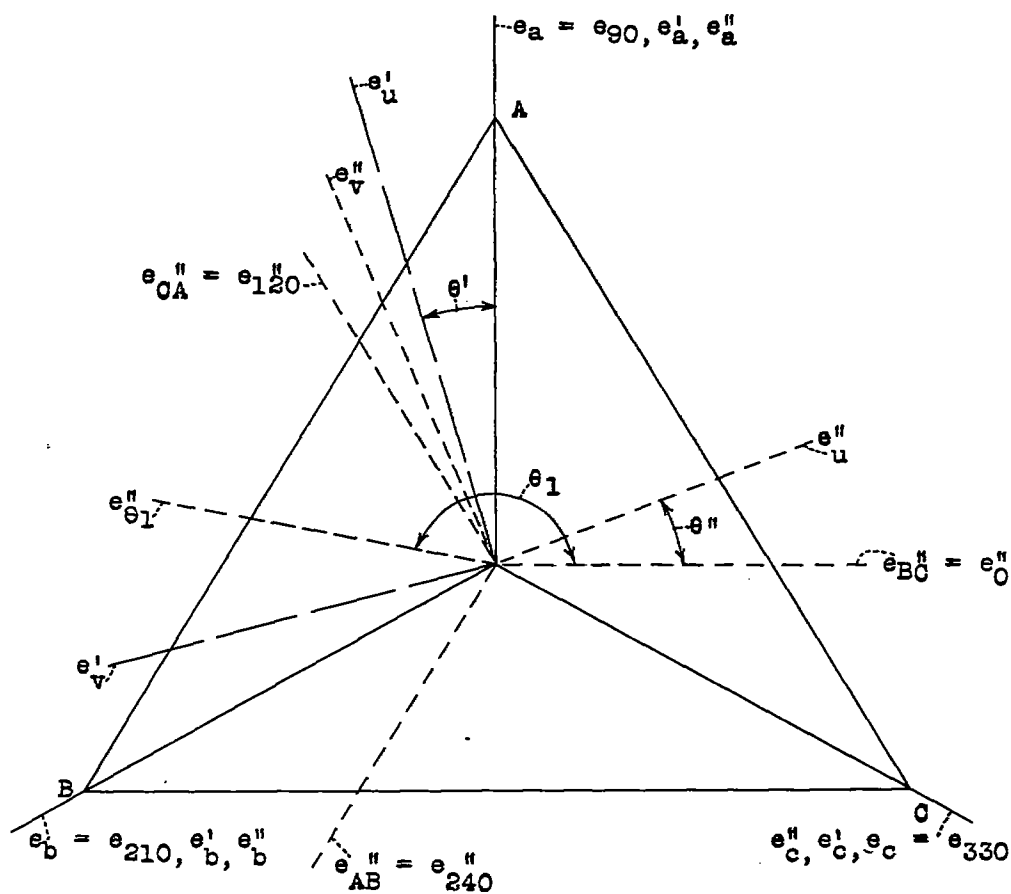


Figure 3.

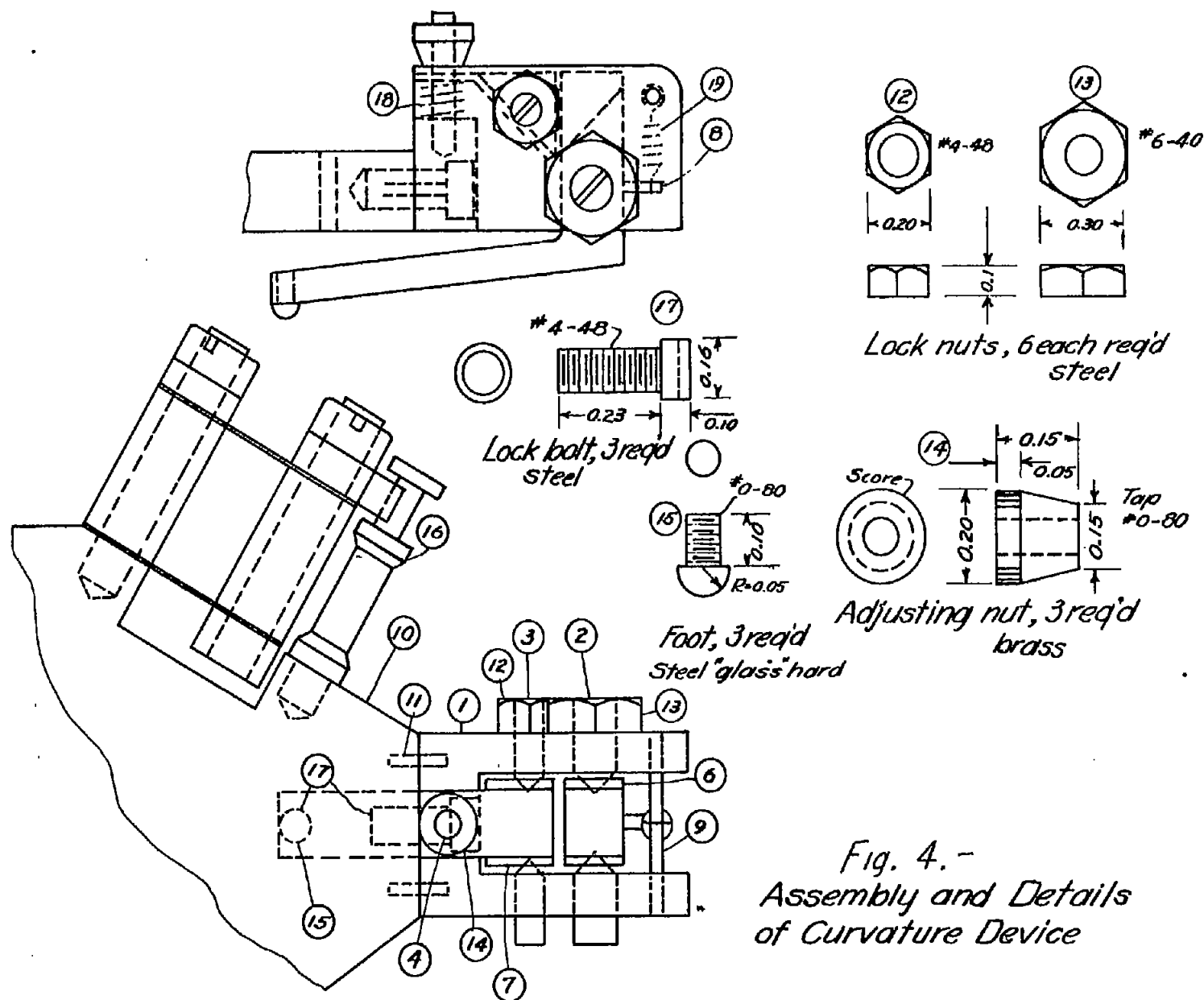


Fig. 4.-  
Assembly and Details  
of Curvature Device



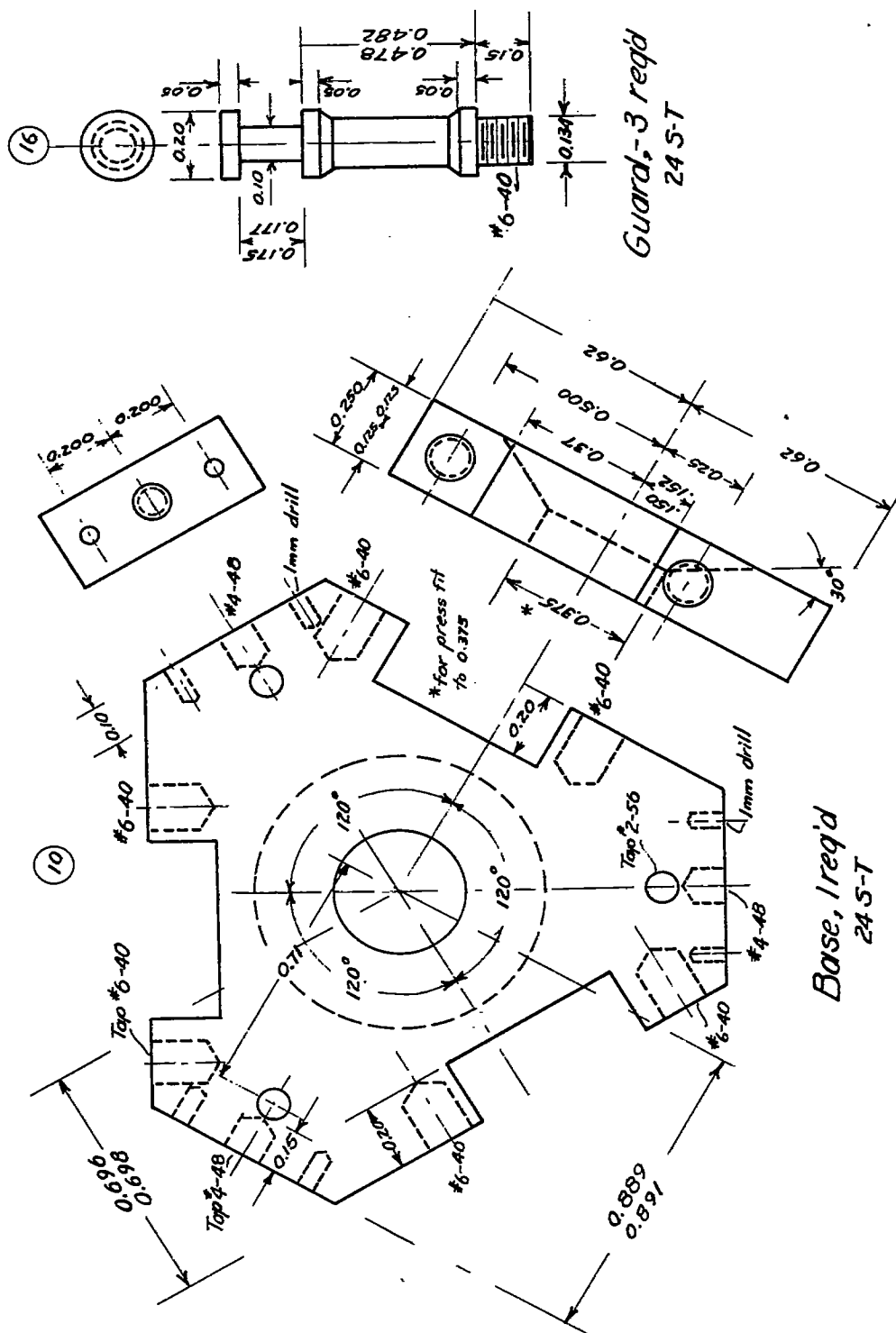
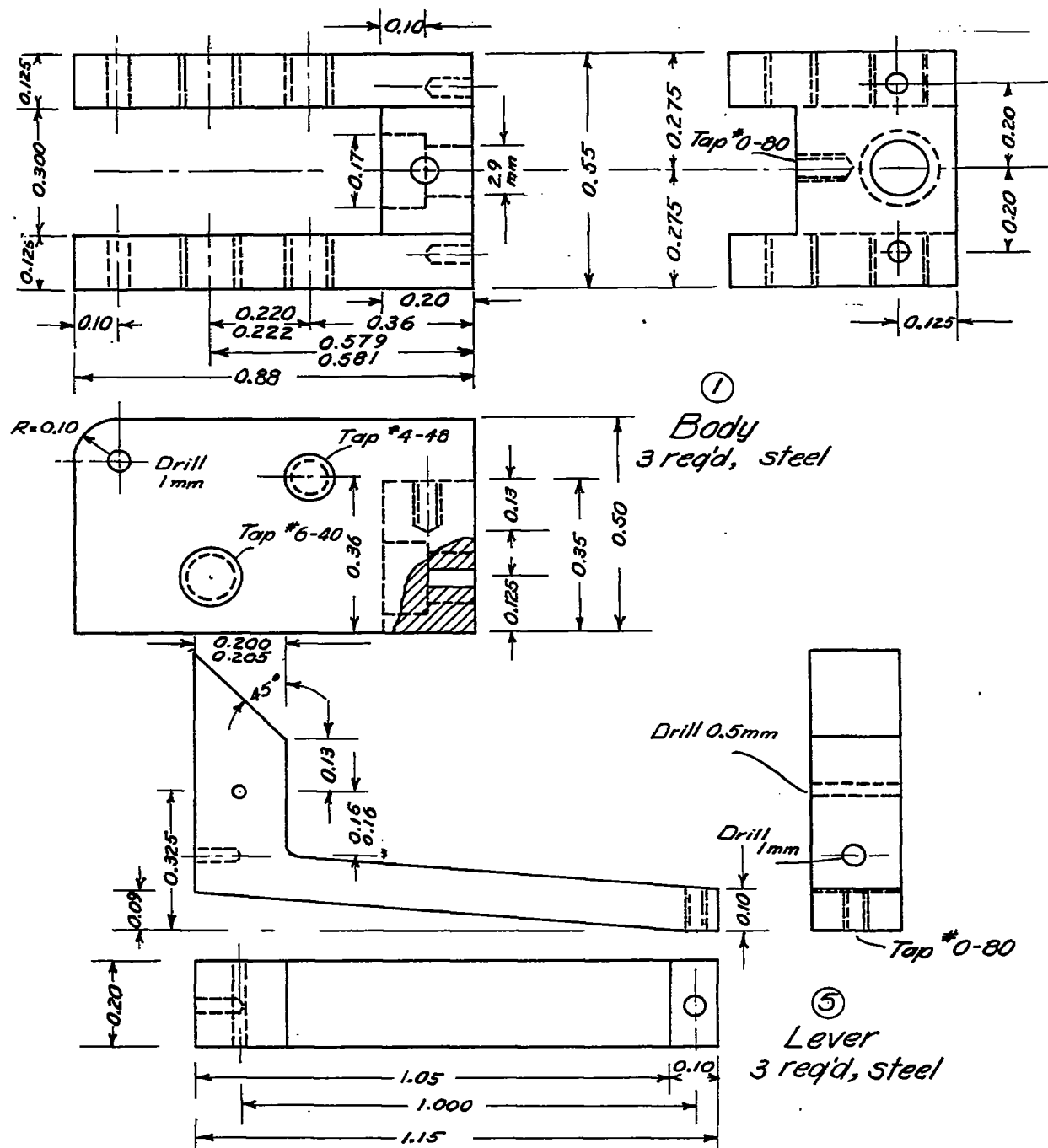


Fig. 5. - Details of Curvature Device

Dimensions in inches except where noted  
Limits as noted others ± 1 in last figure



*Dimensions in inches except where noted.*

*Fig. 6. - Details of Curvature Device*

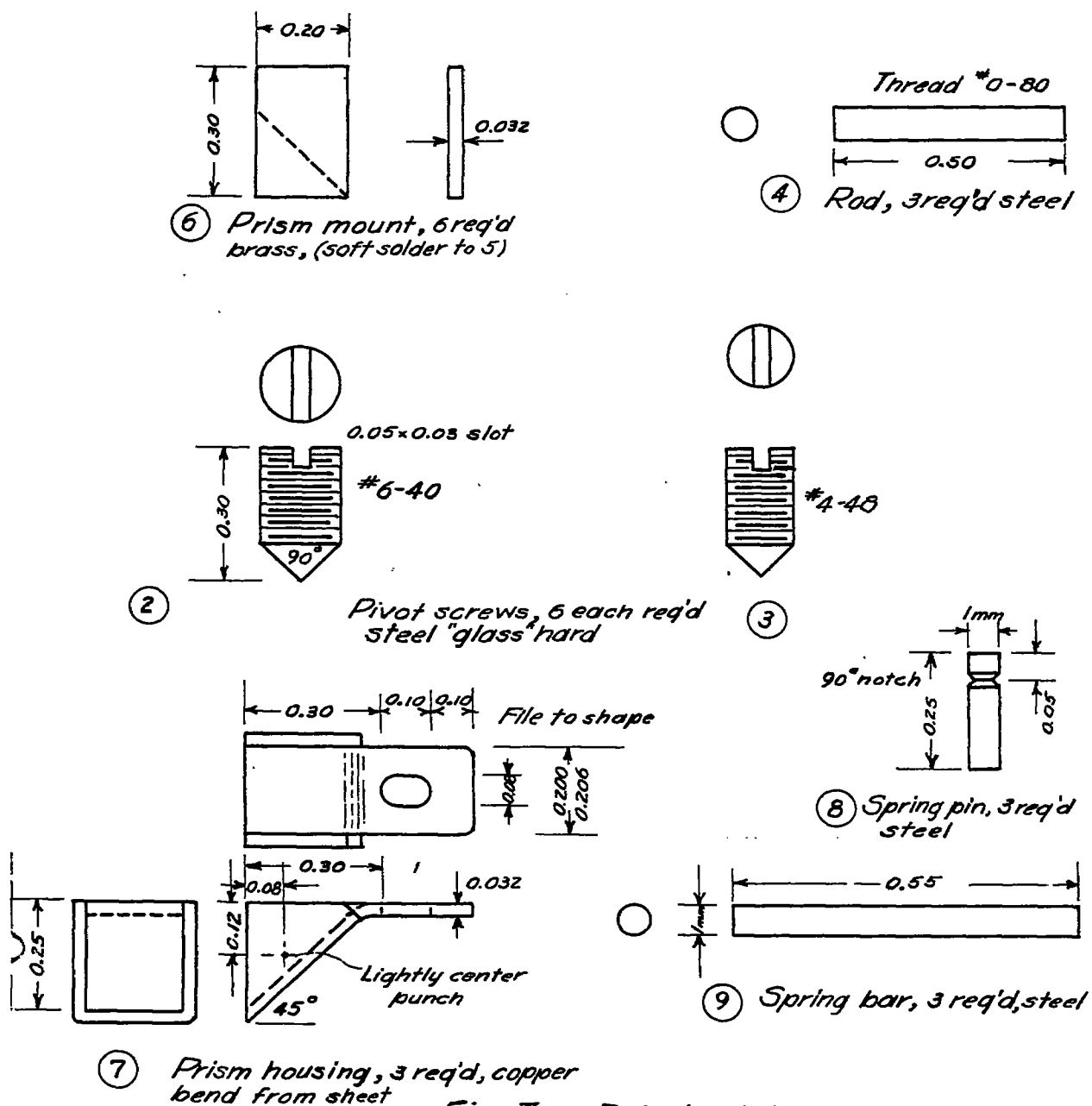


Fig. 7. - Details of Curvature Device

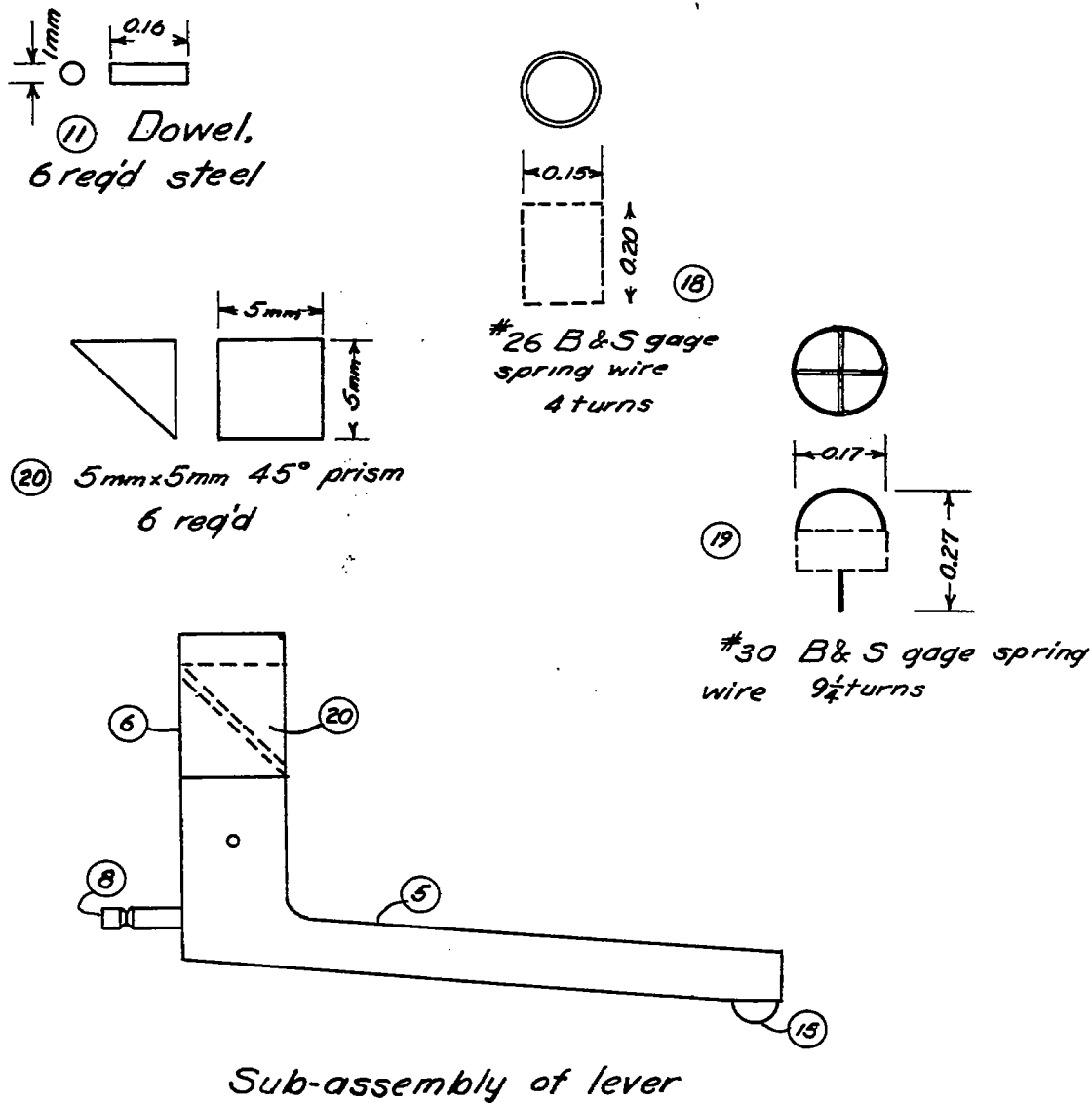


Fig. 8. - Details of Curvature Device

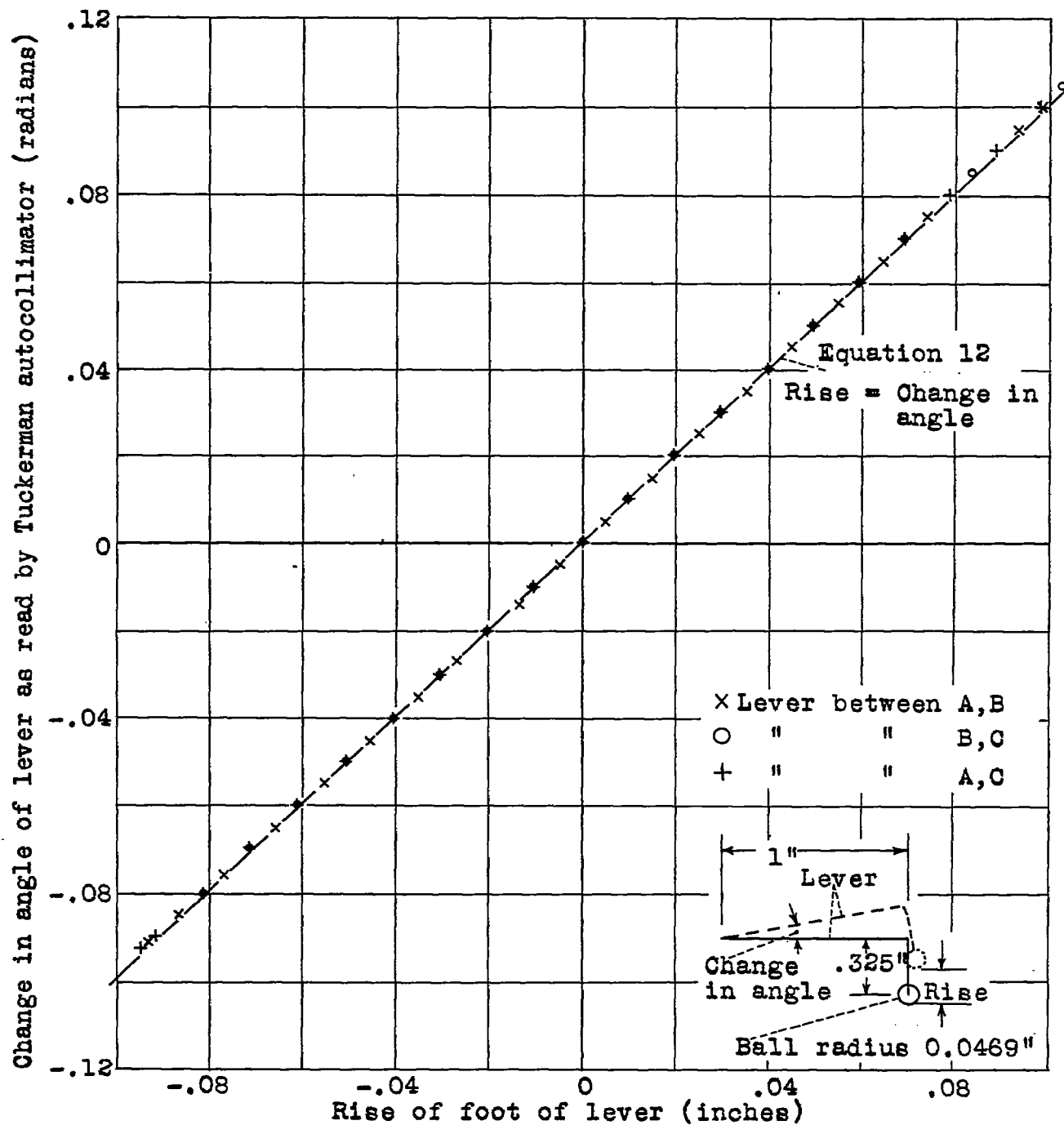


Figure 9.- Calibration of levers.

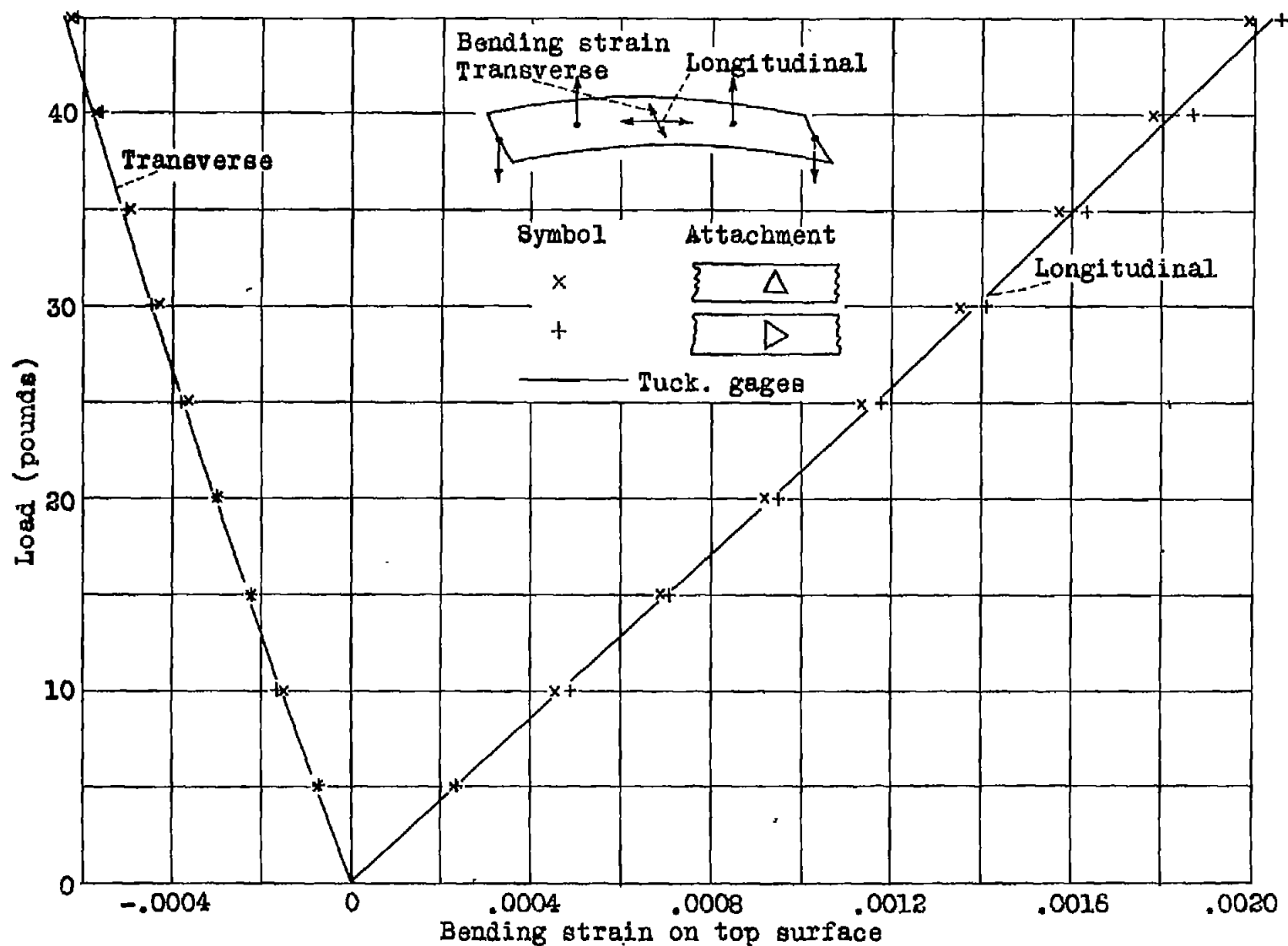


Figure 10.- Comparison of bending strain measured by Tuckerman gages and by curvature device for bent-strip.

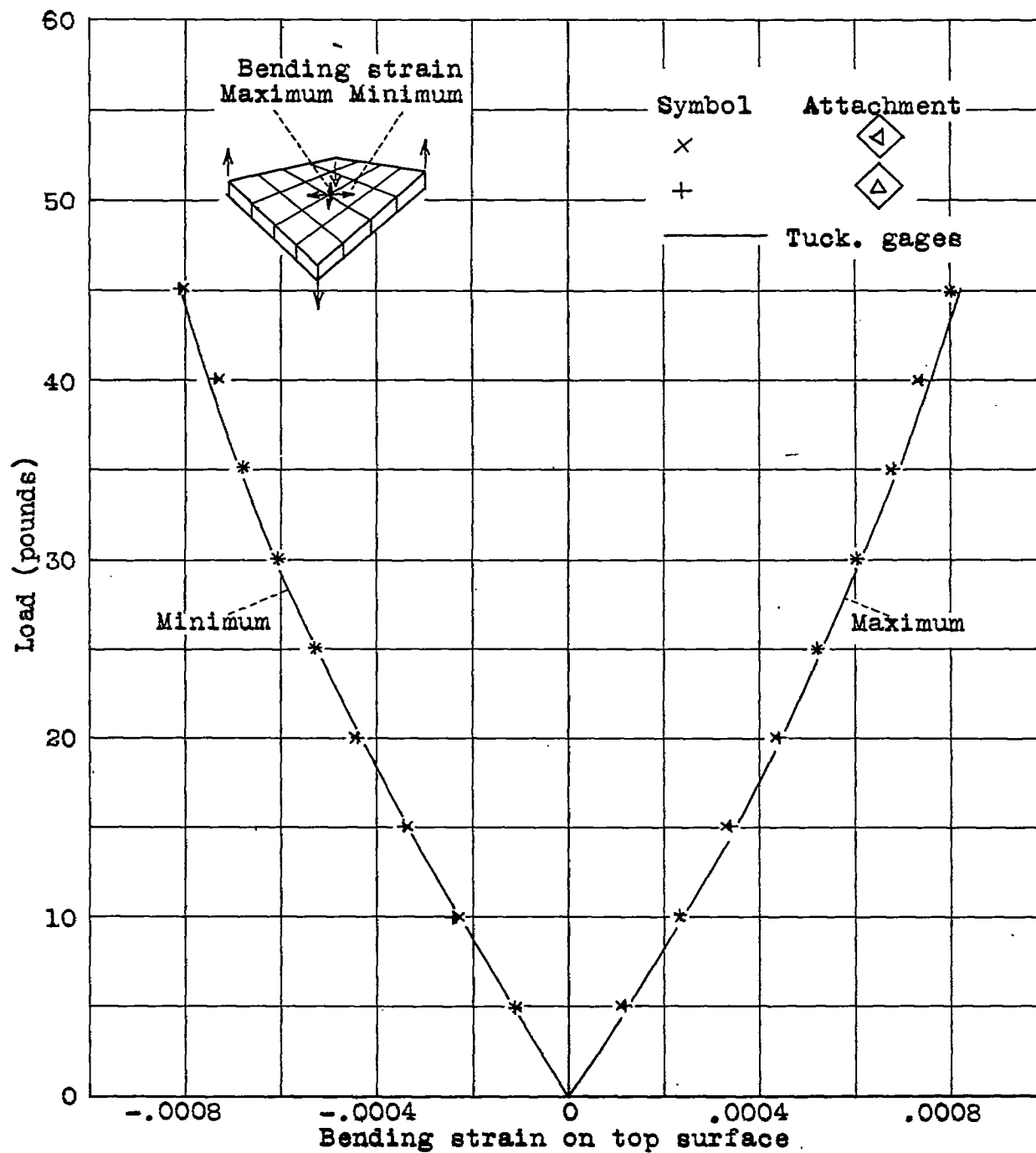


Figure 11.-- Comparison of bending strain measured by Tucker-man gages and by curvature device for saddle plate.